DEVELOPMENT OF A MATHEMATICAL MODEL FOR THE ENERGY BALANCE OF THE LASER CLADDING PROCESS OF METALLIC POWDERS WITH A COAXIAL NOZZLE

YEVHEN KARAKASH[1], MIROSLAV RIMAR[2], OLENA KARPOVYCH[3], DENYS ZHUMAR[3], JAN KIZEK[2], MARCEL FEDAK[2], ANDRII KULIKOV[2]

[1]Industrial and Business Technologies, Ukrainian State University of Science and Technologies, Dnipro, Ukraine

[2]Technical University of Kosice, Faculty of Manufacturing Technologies with a seat in Presov, Presov, Slovak Republic

[3]Oles Honchar Dnipro National University, Physical and technical faculty, Dnipro, Ukraine

DOI: 10.17973/MMSJ.2024_03_2023152

e-mail: jan.kizek@tuke.sk

Modern technologies require innovative solutions for producing complex structures from various materials. Additive manufacturing (AM) or 3D printing presents such a challenge and has significantly impacted the environment across manufacturing sectors, regardless of size. Researchers and technicians have developed new design approaches by exploring fundamental components, materials, and manufacturing processes beyond traditional frameworks, addressing global complex material and design challenges. Laser cladding of metal powders with a coaxial nozzle is one such technology, offering highly productive processes for large-scale component production. Fiber lasers are optimal for providing laser radiation, ensuring required emission quality and stability. The authors seek to develop a mathematical model for the energy balance of coaxial laser cladding of metal powders, aiming to provide an overview of energy consumption levels and unit characteristics for powder delivery, inert gas, and laser radiation sources in direct metal powder coating setups.

KEYWORDS

Additive manufacturing, bimetallic construction, mathematical model, powder material, melting

1 INTRODUCTION

Modern times require modern technologies and new materials that enable the production of higher-quality products. The development of new materials progresses with the development of new technologies. The development in the field of materials is not only focused on developing new materials but also on their protection, as presented by the authors in the work [Sukhodub 2019]. Waste recycling technologies also play an important role here [Holubcik 2020, Zajemska 2022 and 2023], where their energy value also plays a significant role. In the search for more advanced materials, it is necessary to overcome many obstacles that can simultaneously serve as research goals. The properties of new materials are investigated in detail because of their use in practice or for technologies where they will be used in powder form [Onuike 2018, Sebek 2017]. The magnetic properties of materials are significant [Oleksakova 2017 and 2022, Slovensky 2020, Miglierini 2006], which are important in many branches of industry. However, the energy demand and efficiency of each technology remain the basis.

In the article, the authors focused on technologies using Lasers, which are among the progressive technologies that enable high-quality and precise processing of materials. These include e.g. technologies for surface treatment [Sebek 2017], the effect of a laser beam on the material [Panda 2021], or use in welding problematic materials [Behulova 2023] or additive manufacturing process technologies [Bandyopadhyay 2021 and 2022b].

The author's intention in the article is to describe available technologies directly focused on additive manufacturing. The process technology of laser cladding of metal powders with a coaxial nozzle will be described in detail. The goal is to create a mathematical model of the energy balance.

2 TECHNOLOGICAL PROCESSES OF ADDITIVE MANUFACTURING

The development of modern industry requires the production of components with extremely complex geometric shapes using metals, alloys, and bimetallic constructions that can simultaneously meet the needs for high mechanical properties, as well as physical properties [Jandacka 2015 and 2019]. For example, bimetallic combinations of heat-resistant alloys with heat-conductive metals in rocket components. Therefore, additive manufacturing (AM) technologies can serve as a solution to this technological challenge.

Table 1. Advantages and Disadvantages of AM Technologies

Process Method	Advantages	Disadvantages
Powder-based Directed Energy Deposition: DED, DLD, DMD, LMD, LENS	High functionality and built-in functions; Moderate processing speed; Generation of functionally graded material; Processing flexibility; Repair capability	Requires support structure; Typically requires post-processing; Powder handling and environmental impact/safety; Difficulty in recycling mixed powder.
Wire-based Directed Energy Deposition: EBF/EBM, LMWD, WAAM	Capability to manufacture large-scale components; Less material waste; Low material cost: feedstock wire is significantly cheaper than metal powder; Easy material processing and safety.	High energy consumption/thermal control; Low resolution; Low deposition speed; Requires support structure; Requires high material ductility; Needs post-processing; Residual stress/deformation; Melting efficiency.
Powder Bed Fusion (PBF): SLM, SLS	High resolution/ precision and small details; No need for support structures; Fully dense parts; High specific strength and stiffness.	Low build speed; More material waste; Limitation on large size; Powder handling and environmental impact; Difficulty in recycling mixed powder.
Hybrid Additive Manufacturing (HAM)	High dimensional accuracy; Material properties uniformity; High-quality surface finishing; Complex geometries for end-use; Reduced material costs and overall costs.	Not suitable for powder bed melting process; Higher level of automation for manufacturing sequences; Material processability and special clamping; Cooling fluid control and cleanliness during processing.

Modern additive manufacturing (AM) encompasses the following technological processes:

- Powder-based directed energy deposition (DED) technologies: DED, DLD, DMD, LMD, LENS;
- Wire-based directed energy deposition: EBF/EBM, LMWD, WAAM;
- Powder bed fusion (PBF) technology – includes SLM, SLS;
- Hybrid additive manufacturing (HAM).

All these technologies have their advantages and disadvantages. Table 1 summarizes some of the advantages and disadvantages of various AM technologies [Bandyopadhyay 2021,2022a, Onuike 2018].

2.1 *Directed Energy Deposition Technology Based on Powder (DED Technology)*

Powder-based directed energy deposition (DED) technology is a type of metal additive manufacturing (AM) that utilizes a focused laser as the energy source and metallic powder as the raw material. Metallic powders are fed through channels using a carrier gas, usually argon, into the laser focal point. The supplied powders melt at the laser focus point, producing a pool of molten metal. The molten metal quickly solidifies as it moves along a predefined raster scanning trajectory, forming a deposited layer of melted metal. After the first layer is fully deposited, the laser head moves upward along the Z-axis and repeats the powder deposition process over the previous layer until the desired part geometry is completed. The entire working chamber is sealed and usually filled with an inert gas during laser processing, or the molten pool is enclosed to prevent oxidation. Processing parameters such as laser power, powder feed rate, and scanning speed can be adjusted during processing. Dual or multiple powder feeders allow the production of bimetallic/multimaterial additions in a single process. The powder feed rate for each feeder can be individually adjusted during the fabrication of a product, employing different strategies. DED systems can also feature a five-axis processing head, and coaxial nozzle functions enable the application of material layers on complex geometry surfaces [Bandyopadhyay 2016,2018, Traxel 2020, Zhang 2018].

2.2 *Wire-Based Additive Manufacturing Technology (DED)*

Wire-based additive manufacturing (AM) technology using metallic wire is also a variant of DED processing. The energy source for wire-based AM can be a laser, electron beam, or electric/plasma arc. Various wire-based metal AM technologies have been developed based on different energy sources, such as Wire Arc Additive Manufacturing (WAAM), Wire and Laser Additive Manufacturing (WLAM), and Electron Beam Freeform Fabrication (EBF). WAAM and WLAM technologies are the most common. EBF processing requires a vacuum chamber, and EBF-manufactured products usually have stricter dimensional tolerances. The drawbacks of this technology include low deposition speed, high cost, and size limitations imposed by the dimensions of the working chamber [Bandyopadhyay 2022b and 2022c, Liu 2020, Xu 2020].

2.3 *Hybrid Additive Manufacturing (HAM)*

The use of metal AM in critical constructions is often limited by achievable dimensional accuracy, material property uniformity, and surface quality [Mascenik 2020]. In most cases, AM-produced items require further processing, including thermal and mechanical treatments, to relieve residual stresses and improve surface quality. The concept of hybrid additive manufacturing (HAM) combines subtractive techniques or machining with AM technologies into a single system. HAM could be a potential solution for producing high-quality products with tight tolerances and geometric challenges. Additionally, the combination of two processes may help reduce material waste and costs.

2.4 *Layered Powder Fusion Technology (PBF)*

Metal powder-based layered melting technologies (PBF) include Selective Laser Melting (SLM), which uses a laser or electron beam as the energy source to melt metallic powders on a preformed layer. The laser or electron beam scans and melts the powder in the selected area based on the trajectory from the part file. Once the layer is fully formed, the platform with the part descends, and the next layer is applied. Similar to DED technology, the entire working chamber is filled with an inert gas to prevent oxidation during production. Standard PBF systems usually have only one powder feed layer, requiring powder replacement for manufacturing bimetallic parts. Recently developed PBF systems have configurations such as dual powder beds or dual powder feeders, simplifying the production of parts from multiple materials in one process.

3 MATHEMATICAL MODEL OF ENERGY BALANCE

The most promising method for rapid shape formation and prototyping of products is the volumetric (3D) synthesis with coaxial laser cladding of metal powders. This technology allows for the creation of parts of virtually any complexity with high precision. The material properties of parts produced by coaxial laser cladding match or exceed those of traditional technologies. Importantly, 3D synthesis with laser cladding of metal powders allows for rapid changes in material composition by introducing various powders into the melt. This enables the development of hybrid or gradient metal composites.

3.1 *Development of a Mathematical Model for the Energy Balance of the Coaxial Nozzle Laser Cladding Process with Metallic Powders*

The method of layer-by-layer deposition of metallic powder involves the thermal impact of a scanning laser beam on a pre-applied layer. In this case, the thermal conductivity of the powder plays a crucial role, which can be significantly lower than the thermal conductivity of the material of the particles themselves due to the presence of air gaps between them. Ultimately, the air gaps between particles largely determine the thermal conductivity of metallic powders [Ivanova 1998, Panchenko 2010, Shishkovsky 2009]. Additionally, the material's thermal conductivity depends on the melting temperature. The reason is that, under radiation exposure, the particles of the upper layer, directly exposed to the radiation, melt first. The resulting melt can fill the air gaps, thus providing thermal contact between the liquid metal and the layer below. This process continues sequentially down to the lowest layer of particles. The influence of the flow of the liquid phase on the thermal conductivity of the powder during sintering with the addition of components with low melting temperatures, preserving the framework of refractory particles, was studied in [Zhang 1998]. However, due to the presence of a framework of refractory particles, the melt of low-melting components cannot exert the same strong influence on the thermal conductivity of the powder as when melting all its elements. When melting a monopowder, it can be assumed that the value of thermal conductivity is close to the thermal conductivity of the material of the particles.

Consideration of melting is also essential for modeling the absorption of laser radiation by the powder. In the conditions of powder melting, due to the influence of the melt, the surface heat source model is quite adequate to real absorption processes.

The thermophysical properties of the powder material do not depend on temperature and are assumed to be constant and

equal to the values at normal temperature. This assumption is quite acceptable for determining the energy parameters of the process for selecting equipment nodes since the values of power consumed will be maximal.

The total energy balance of power, which takes into account the main channels of energy consumption of absorbed laser radiation, can be determined by the formula [Onuike 2018]:

$$\eta_L P_L = P_\tau + P_T + P_H + P_V \quad (1)$$

Where,

η_L - is the absorption coefficient of radiation;

P_L - is the laser source power; is the power required for melting the powder roll;

P_τ – power required to melt the powder roller

P_T - is the power for melting the upper part lying below the layer or the substrate (for the first layer);

P_H - is the power consumed for heating the liquid phase;

P_V - is the power consumed for evaporation.

Having determined all the components of useful costs on the right side of equation (1) and knowing the absorption coefficient of radiation, it is possible to determine the power of the laser source.

The power for melting the powder roll is given by:

$$P_\tau = \rho_0 d_0 h V (c_p T_t + H_T) \quad (2)$$

where,

ρ_0 - is the density of the material of the particles;

d_0 - is the diameter of the laser beam on the powder surface;

h - is the thickness of the powder roll;

V - is the scanning speed of the laser beam (melting speed);

c_p - is the specific heat;

T_t, H_T -is the melting temperature and the specific energy of melting of the material of the powder particles.

The power PT for melting or for sufficiently heating the upper part lying below the layer is determined from the condition of linear approximation of the temperature distribution in depth:

$$P_T = \frac{1}{2}\rho_0 d_0 V (h_t - h) c_p T_t \quad (3)$$

where,

$h_t - h = \Delta h$ - is the depth of penetration of the temperature wave into the formed layer;

h_t - is the total depth of melting. The parameters Δh and h_t are undetermined and require a preliminary calculation of temperature fields during the cladding of a roll of the required thickness.

The power consumed for heating the liquid phase can be estimated by the formula:

$$P_H \approx \frac{1}{2}\rho_0 h d_0 V c_p (T_0 - T_t) \quad (4)$$

Power consumption for evaporation:

$$P_V = m_V H_V \quad (5)$$

where,

m_V - is the mass of the powder evaporating per unit time;

H_V - is the specific energy of evaporation.

The mass flow rate 'M' of the dispenser can be determined by the formula:

$$M' = \frac{\pi k_P d_0 h V \rho_0}{4 k_D} \quad (6)$$

where,

k_D - is the powder utilization coefficient, taking into account the divergence of its flow and other technical factors;

k_P - is the porosity coefficient.

The analysis of the energy balance of power for coaxial laser cladding of metallic powders showed that to determine the powers P_τ, P_T, P_H - it is necessary to determine Δh based on a preliminary calculation of temperature fields during the cladding of a roll of the required thickness. Then, calculate the power consumption for evaporation and determine the power of laser radiation from formula (1).

Using formula (6), the mass flow rate of the dispenser or, with a known value of M' and other given parameters, the possible value of the thickness of the deposited roll h is determined.

4 DETERMINATION OF LASER POWER AND FEEDER MASS FLOW RATE

The laser power required for the laser cladding process of Inconel 718 metallic([SMC 2017]) powder can be determined from formula (1). Initially, it is necessary to determine the components of the energy balance equation: P_τ – power required for melting the powder roll; P_T – power for melting the upper part lying below the layer or the substrate (for the first layer); P_H – power consumed for heating the liquid phase; P_V – power consumed for evaporation. The thermophysical characteristics of the Inconel 718 alloy are presented in Table 2. Data on the latent heat of melting and evaporation of the Inconel 718 alloy are not available in the literature. Therefore, for the calculation, nickel data, as the material with the highest percentage composition, is used:

- latent heat of melting is 302 kJ/kg;
- latent heat of evaporation is 6376 kJ/kg.

The cladding speed is assumed to be 30.103 m/s.

The calculation results are presented in Table 2.

Table 2. Values of components of the energy balance

Energy balance component	Value, W
P_τ	108.5
P_T	18.3
P_H	44.4
P_V	78
$\sum P$	249.2

Assuming the absorption coefficient of radiation $\eta_L = 0.5$, the laser power is given by:

$$P_L = \frac{\sum P}{\eta_L} = \frac{249.2}{0.5} = 498.4$$

Thus, to ensure the cladding process, a laser source of at least 500 W is required.

To determine the mass flow rate M' of the feeder using formula (5), values of the powder utilization coefficient k_D and porosity coefficient (density of material in the part) k_P are required. According to literature data [Stavertiy 2017], the maximum value of the coefficient k_C for coaxial cladding is 0.7. For the calculation, k_C is taken as 0.5, providing a reserve for powder feed regulation.

The porosity coefficient (density of material in the part) k_P for coaxial cladding is assumed to be 0.97.

As a result of the calculation using formula (6), the mass flow rate of the feeder is:

$$M' = 187.3 \times 10^{-6}\, kg/s = 11.2\, g/min$$

In additive manufacturing of parts by coaxial nozzle cladding, the following tool movement speeds are applied [12]:

creating coatings from 5×10^{-3}m/s to 35×10^{-3}m/s;

manufacturing volumetric parts from 3×10^{-3}m/s to 15×10^{-3} m/s

For the minimum process speed, the mass flow rate of the feeder will be 10 times lower than the calculated M'=1.12 g/min. Based on the analysis of literary and calculated data, the feeder should provide a powder mass flow rate in the range of 1.12 g/min to 11.2 g/min. To compensate for powder consumption for

evaporation and other accompanying phenomena of the process, the Powder Feeder PF 2/2 can be used with a range from 0.5 g/min to 15 g/min.

5 COMPARATIVE THEORETICAL STUDIES OF TEMPERATURE FIELDS IN LASER CLADDING OF A SINGLE ROLL ON A SUBSTRATE AND HEATING OF POWDER LAYER IN TRANSPORTING GAS

5.1 Development of a Physical and Mathematical Model for Laser Beam Heating of Powder Layer in Gas Flow

A physical model is proposed for the heating of powder particles by a laser beam while moving in a gas flow. Numerous theoretical and experimental studies of gas flows with particles in a coaxial nozzle during laser cladding have been conducted. The research results indicate that the particle flow in the beam's action area has the shape of an internal cone (Figure 1), the angle of which corresponds to the angle of the channels in the coaxial nozzle. The particle velocity in this region is 1.5 to 2 m/s.

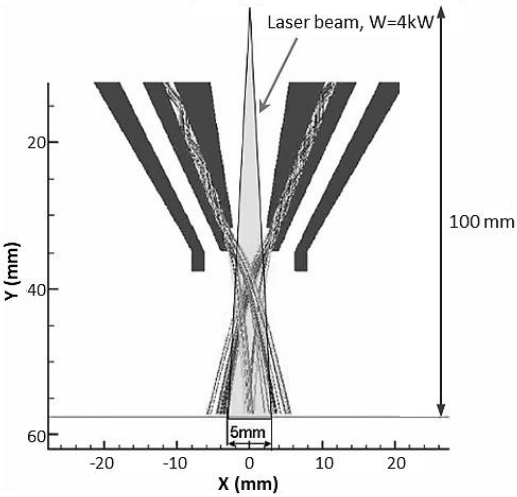

Figure 1. Particle flow in the beam's action area

Assuming that the particle flow is laminar, it is possible to determine the time for the formation of a new layer, which will depend on the particle diameter:

$$t_C = \frac{d_P}{v_P} \quad (7)$$

where,

t_C - is the layer formation time, s; d_P - is the particle diameter, m; v_P - is the particle velocity, m/s.

The laser beam will always act on the newly formed layer. The previous layer, heated to a certain temperature by laser radiation, will move further towards the substrate without heat exchange with other layers. The particle movement time to the substrate can be determined by the formula:

$$t_{sub} = \frac{S}{v_P} \quad (8)$$

where,

t_{sub} - is the particle movement time to the substrate, s; S - is the distance to the substrate, m. Obviously, the layer formation time and the time for heating the particles to a temperature in the range from the melting temperature T_{melt} to the boiling temperature T_{boil} should be less than the particle movement time to the substrate.

Assuming a particle velocity of 1.5 m/s and boundary sizes of powder particles of 50 µm = 0.05×10^{-3} m and 100 µm = 0.1×10^{-3} m, the layer formation time will be 0.03×10^{-3} s and 0.06×10^{-3} s, respectively.

Applied to the cladding of Inconel 718 alloy on a substrate located at a distance of 7 mm = 7×10^{-3} m from the nozzle, the movement time of the heated particle layer to the substrate will be 4.6×10^{-3} s.

To determine the heating time of the particle layer to the required temperature, additional studies are needed. Numerical experiments were conducted for Inconel 718 alloy. A non-stationary heating process of a cone-shaped layer under the influence of a 1 mm diameter laser beam with a power of 500 W was considered (Figure 2).

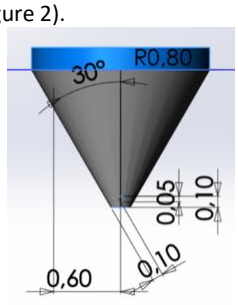

Figure 2. Powder layer of 100 µm particles

Taking into account the reflection coefficient of nickel's radiation as 0.7, the heat flux amounts to 1.9×108 W/m². During the 4.6×10^{-3} s movement time to the substrate, the layer of 100 µm particles on the lower surface contacting the substrate has a temperature below the melting temperature $T_{melt} = 1609K$ (Figure 3).

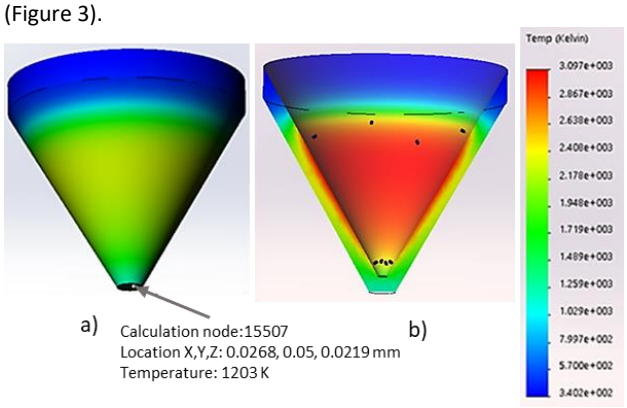

Figure 3. Temperature distribution in a layer of 100 µm particles: a – on the lower surface; b – in the axial section of the layer

The heating time of the lower surface to T_{melt} is approximately 5×10^{-3} s. On the beam-affected surface, the temperature exceeds the boiling temperature $T_{boil} = 3218K$, and some material will evaporate. The heating time of the 100 µm layer throughout the section exceeds the particle movement time to the substrate, and particles at the cone's apex will not be fully melted, failing to form a strong bond on the substrate or a previously formed layer. For 50 µm particles, the heating time of the lower surface of the layer is 2.8×10^{-3} s, which is less than t_C and t_{sub}, and the particles will fully melt (Figure 4).

Based on the conducted studies, it can be concluded that when forming a powder layer with particle sizes ranging from 50 to 100 µm, under the influence of a 500 W laser beam and a particle velocity of 1.5 m/s in the gas flow, not all particles will be fully melted at the moment of deposition on the substrate. In this case, the powder mass flow rate should be 15.3 g/min, and the cladding speed should be 40 mm/s for a 0.5 mm thick layer.

According to the selected equipment, the maximum powder mass flow rate is 11 g/min, corresponding to a layer formation time of 3.6×10^{-3} s for 50 µm particles and 7.2×10^{-3} s for 100 µm particles. Therefore, to achieve complete melting of 100 µm particles, it is necessary to reduce the powder mass flow rate or the particle velocity in the flow.

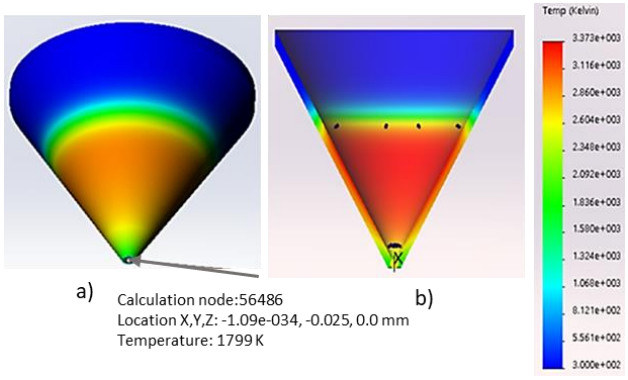

Figure 4. Temperature distribution in a layer of 50 µm particles: a – on the lower surface; b – in the axial section of the layer

These calculations need experimental verification. The calculation results also revealed that an extensive heat source, in the form of a melted layer, with non-uniform temperature distribution across the radius and thickness, acts on the substrate or a previously formed layer. In the next stage of modeling the laser cladding process of Inconel 718 alloy powder, it is necessary to conduct step-by-step studies of temperature fields on the substrate, taking into account the movement speed of this source. This will allow simulating the process of roller formation and determining the cooling time to 1000 K. It is also necessary to consider the movement of gas flows from the coaxial nozzle to the substrate, determine the size of the protected zone, and calculate the time to ensure conditions for protecting the formed surface, which should be equal to or greater than the cooling time.

5.2 Investigation of Temperature Fields in Laser Cladding of a Single Roller on a Substrate

Mathematical analysis of temperature fields during the cladding of a single roller on a substrate was carried out for Inconel 718 alloy. The thermal properties of this alloy are presented in Table 3. [SMC 2017]

Properties	Inconel 718
Density, kg/m³	8.2×10³
Melting Temperature, °C (K)	1336 (1609)
Boiling Temperature (Calculated $T_{boil} = 2\ T_{melt}$), °C (K)	2672 (3218)
Thermal Conductivity, W/(m·K)	11.4
Specific Heat, J/(kg·K)	435
Thermal Diffusivity, m²/s	3.2×10⁻⁶

Table 3. **Thermal Properties of Inconel 718 Alloy [SMC 2017]**

The geometric dimensions of the roller and substrate are shown in Figure 5.

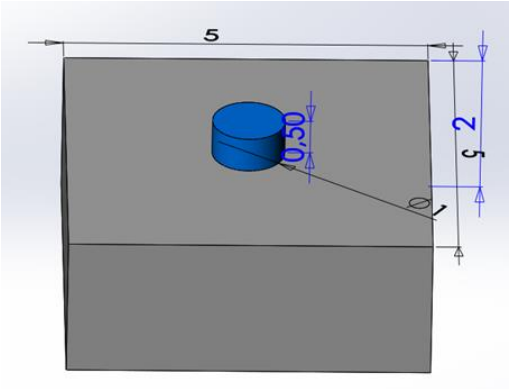

Figure 5. Geometric model of a single roller and substrate

The dimensions of the roller correspond to the assumed cladding parameters with a typical laser beam interaction time on the deposited metal, $t_m = d_0/V$, determined by the laser beam diameter $d_0 = 1mm$ and roller thickness $h = 0.5mm$. The substrate dimensions were chosen to maximize adherence to the assumption of surface heat source influence.

The material of the substrate is also assumed to be Inconel 718 alloy.

Thermal calculations were conducted using SolidWorks with the following boundary conditions:

- the temperature on the roller's surface was set to T_{boil};
- the temperature on the lower surface of the substrate was 293 K;
- the heat transfer coefficient on the contact surfaces between the roller and the substrate was not considered, assuming global contact.

Both steady-state and transient calculations were performed with the laser beam temperature influence on the roller surface, T_{boil}, applied for 1 s (Figure 6).

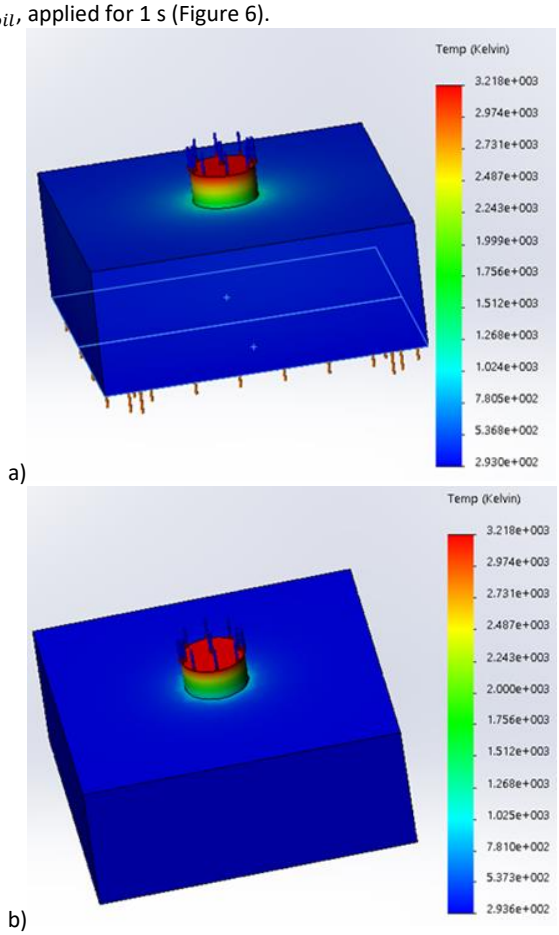

Figure 6. Results of temperature field calculations: a – steady-state calculation; b – transient calculation

The analysis of the results revealed that the temperature on the contact edge between the roller and the substrate is lower than $T_{melt} = 1609K$ in both cases. Consequently, no melting of the deposited material with the substrate will occur in this zone. The temperature distribution in the central section of the model in the contact zone of the lower surface of the roller with the substrate is uneven (Figure 7).

According to the results of the steady-state calculation, the non-melting zone is 0.5(d_0/2) = 0.25 mm; thus, the adhesion of the roller to the substrate occurs over a diameter length of 0.5 mm. In the transient calculation, there are no temperatures at the contact between the roller and the substrate equal to or higher than T_{melt}. Theoretical analysis showed that to increase the area of material melting with the substrate or the previous layer, it is

necessary to create temperatures on the surface of the cladded roller equal to or exceeding the T_{melt} of the material. Therefore, evaporation is a crucial factor for quality cladding, which needs to be considered in determining the mass supply of metal powder and laser beam power calculation.

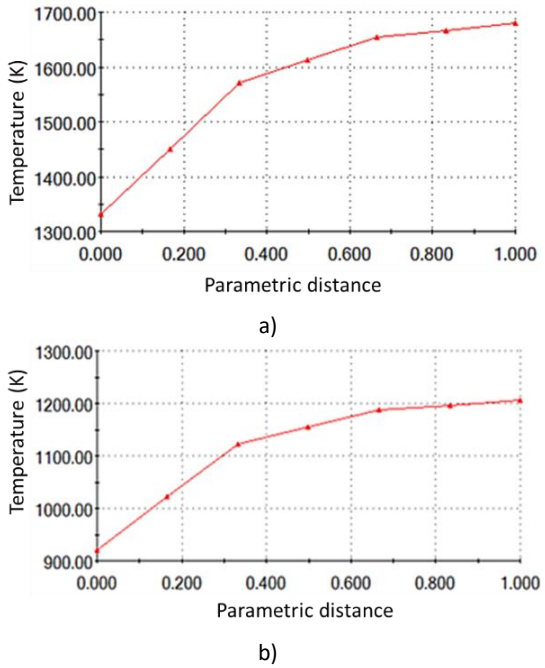

Figure 7. Temperature distribution along the radius of the roller in the central section a – steady-state calculation; b – transient calculation

To determine the power value P_T using formula (3), the depth of penetration of the temperature wave into the formed layer Δh is needed. According to the results of the steady-state calculation, its value along the axis of the cladded roller is approximately 0.03 mm (Figure 8).

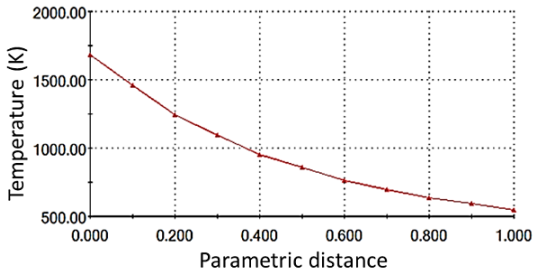

Figure 8. Temperature distribution along the height of the substrate in the central section

Theoretical studies of temperature field distribution in the cladding zone of a single volume of a roller made of Inconel 718 alloy powder on a substrate have shown the necessity of creating a temperature on the surface of the cladded roller equal to or exceeding the T_{melt} of the material. Evaporation is a crucial factor for quality cladding, which needs to be considered in determining the mass supply of metal powder and laser beam power calculation.

5.3 Comparative Analysis of Theoretical Studies

A comparative analysis of the results of theoretical studies of temperature fields during laser cladding of a single roller on a substrate and heating of a powder layer in a gas flow revealed the following:

For the considered physical and mathematical models of heating a powder layer with laser radiation, the temperature fields significantly differ:

During the heating of a single volume directly on the substrate, the maximum temperature is located in the central region, and on the periphery, its value does not reach the melting temperature (T_{melt}) of the material.

Heating a cone-shaped powder layer, while moving in a gas flow towards the substrate, results in the maximum temperature occurring on the periphery and the minimum in the center of the layer [Kuznetsov 2020].

The interaction of the powder flow with laser radiation requires experimental verification.The heated powder layer can be considered as a heat source with non-uniform temperature distribution in the radial direction and can be used in modeling the formation of the roller.

These findings highlight the importance of experimental validation for the interaction between the powder flow and laser radiation. Additionally, the heated powder layer's characteristics as a heat source should be considered in modeling the formation of the roller during the laser cladding process.

6 DEVELOPMENT OF A PHYSICAL AND MATHEMATICAL MODEL OF GAS FLOWS IN A TRIPLE COAXIAL NOZZLE

The model of the triple coaxial nozzle was created using the SolidWorks software (Figure 9). Geometric parameters were chosen based on literature data for this type of nozzle.

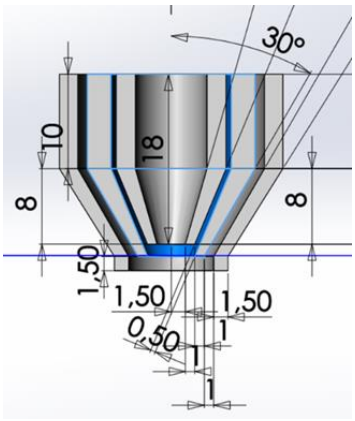

Figure 9. Geometric model of the nozzle: axial section and geometric parameters of the nozzle

The following mass flow rates in the channels were taken as initial data:

- axial flow – $Q_1 = 0.11\times10^{-3}$ kg/s;
- transporting flow – $Q_2 = 0.16\times10^{-3}$ kg/s;
- protective external flow – $Q_3 = 0.54\times10^{-3}$ kg/s.

Gas flow simulation in the nozzle channels was performed using the Ansys software. Based on the nozzle model, the calculation zone was determined, and channels were formed to define the surfaces of gas flow inlet and outlet (Figure 10).

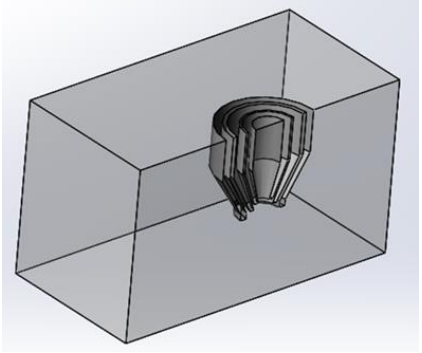

Figure 10. Geometric model of the nozzle: axial section – channels and calculation zone

The task was solved with the following assumptions:

- The task is solved in a 3D setup with a Symmetry constraint.
- Subsonic gas flow with consideration of non-stationary processes is considered.
- Turbulence model – Standard k-ε; flowing medium – argon gas.

As a result of the calculation, the flow velocities in the channels, streamline patterns, pressure distribution, and density in the calculation domain were determined (Figs. 11 – 14).

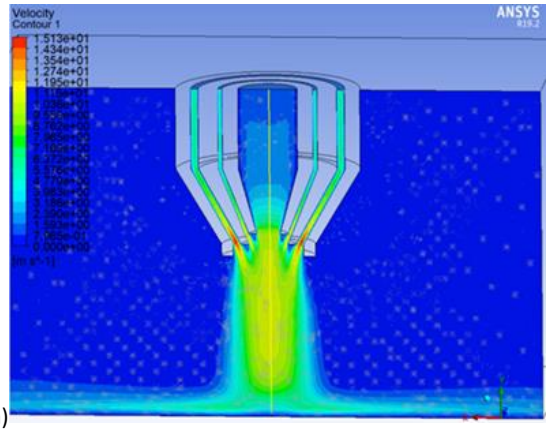

a)

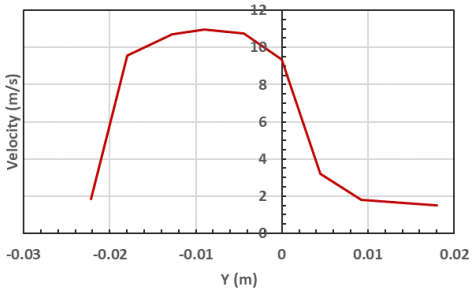

b)

Figure 11. Velocity distribution: a – velocity distribution in the channels; b – flow velocity along the axis in the central channel

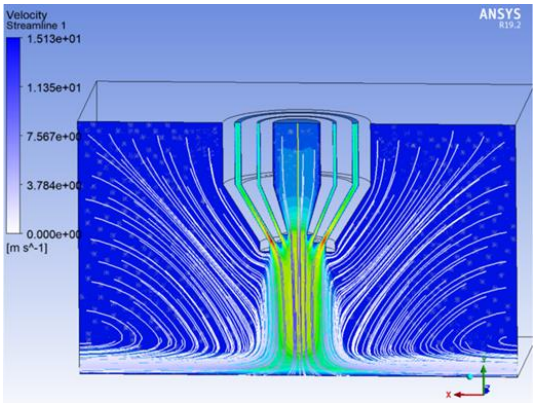

Figure 12. Streamlines in the calculation domain

Based on the calculations, the following conclusions can be drawn:

- Flow velocities in the central part of the flow domain equalize.
- In the central part, the flow velocity reaches 12 m/s, while at the periphery, the velocity decreases to 4 m/s.
- The area on the substrate protected by the gas flow is not more than one nozzle diameter from the nozzle axis. In other words, the size of the protected area is equal to 2 times the nozzle diameter (2d nozzle).

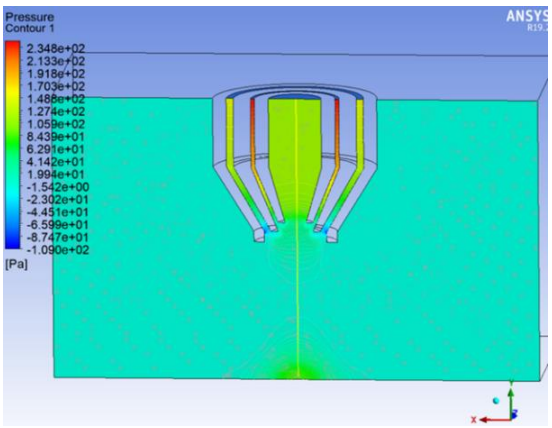

Figure 13. Pressure distribution in the calculation domain

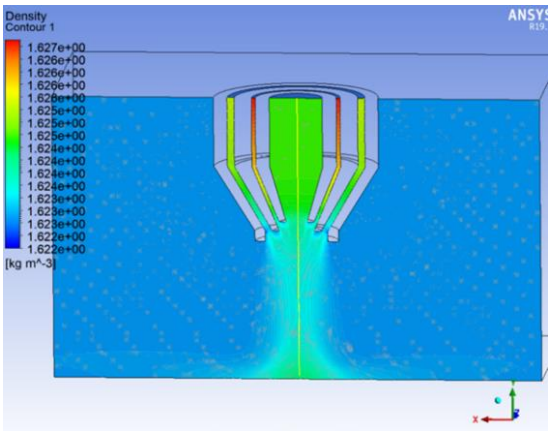

Figure 14. Density distribution in the calculation domain

7 CONCLUSIONS

The conducted research leads to the following conclusions:

Laser processing of powder materials using a coaxial nozzle is a high-productivity process suitable for manufacturing large-sized components.

Fiber lasers are the most appropriate source of laser radiation, ensuring the required quality and stability of emission.

The energy balance of coaxial laser cladding of metal powders includes various components: $\boldsymbol{P_\tau}$ – power for melting the powder roll; $\boldsymbol{P_T}$ – power for melting the upper part lying below the layer; $\boldsymbol{P_H}$ – power for heating the liquid phase; $\boldsymbol{P_V}$ – power for vaporization.

Numerical analysis of the power balance in the coaxial cladding process of Inconel 718 alloy powder revealed a total power consumption of $\sum \boldsymbol{P} = \boldsymbol{249.2\ W}$ and the required power of the fiber laser, which should be at least 500 W.

The mass flow rate of the powder feeder was determined, considering the applied speeds of the technological tool movements. For additive manufacturing of components using coaxial cladding, the Powder Feeder PF 2/2 with a range from 0.5 g/min to 15 g/min can be employed.

An algorithm for determining the energy balance of the laser cladding process of metal powders includes several stages:

- defining the initial data of the coaxial cladding process – geometric parameters of the deposited layer, laser beam diameter;
- determining the thermophysical and optical properties of the deposited material;
- calculating temperature fields to establish the depth of substrate melting or the previously formed layer;
- determining the components of the energy balance and the total power of the laser cladding process;

- determining the power of the laser radiation source.

This algorithm does not allow for a complete analysis of all physical processes occurring in coaxial laser cladding of powder materials. Still, it provides insight into the level of energy consumption and characteristics of the units and components for the powder delivery system, inert gas, and the laser radiation source in the direct metal powder cladding setup.

Comparative analysis of theoretical studies on temperature fields during laser cladding of a single roll onto a substrate and heating of a powder layer in a gas flow showed significant differences in temperature fields for the considered physical and mathematical models. Experimental verification is required.

The heated powder layer can be considered as a heat source with non-uniform temperature distribution in the radial direction and can be used in the modelling of roll formation.

Numerical simulation of gas flows in the triple coaxial nozzle allowed determining flow parameters and the area protected by inert gas during cladding.

Flow velocities in the middle part of the flow domain equalize. In the central part, the flow velocity reaches 12 m/s, while at the periphery, the velocity decreases to 4 m/s.

The area on the substrate protected by the gas flow is not more than one diameter of the outlet section from the nozzle axis, meaning the size of the protected area equals 2 times the nozzle diameter (2dnozzle).

ACKNOWLEDGMENTS

This article was supported by the state grant agency for supporting research work and co-financing within the project KEGA 024TUKE-4/2024.

REFERENCES

[Bandyopadhyay 2016] Bandyopadhyay, A. and Bose, S. Additive Manufacturing. Boca Raton: CRC Press, Boca Raton, 2016. ISBN 978-1-4822-2360-6

[Bandyopadhyay 2018] Bandyopadhyay, A. and Heer, B. Additive Manufacturing of Multi-Material Structures. Materials Science and Engineering: R: Reports, 2018, Vol. 129, pp. 1-16.

[Bandyopadhyay 2021] Bandyopadhyay, A., Traxel, K.D. and Bose, S. Nature-inspired Materials and Structures Using 3D Printing. Materials Science and Engineering: R: Reports, 2021, Vol. 145, 100609.

[Bandyopadhyay 2022a] Bandyopadhyay, A., Zhang, Y., and Onuike, B. Additive manufacturing of bimetallic structures. Virtual and Physical Prototyping, 2022, Vol. 17, No. 2, pp. 256-294.

[Bandyopadhyay 2022b] Bandyopadhyay, A., Bose, S. and Narayan, R. Translation of 3D-Printed Materials for Medical Applications. MRS Bulletin, 2022, Vol. 47, No. 1, pp. 39-48.

[Bandyopadhyay 2022c] Bandyopadhyay, A., et al. Alloy Design via Additive Manufacturing: Advantages, Challenges, Applications and Perspectives. Materials Today, 2022, Vol. 52, pp. 207-224.

[Behulova 2023] Behulova, M. and Babalova, E. Numerical Simulation of Temperature Fields during Laser Welding–Brazing of Al/Ti Plates. Materials, 2023, Vol. 16, No. 6, 2258.

[Holubcik 2020] Holubcik, M., Klackova, I., Durcansky, P. Pyrolysis Conversion of Polymer Wastes to Noble Fuels in Conditions of the Slovak Republic. Energies, 2020, Vol. 13, 4849. https://doi.org/10.3390/en13184849.

[Ivanova 1998] Ivanova, A.M., et al. Physical features of selective laser sintering of powder metal-polymer compositions. Quantum Electronics, 1998, Vol. 25, No. 5, pp. 420-425.

[Jandacka 2015] Jandacka, J., et al. The Increase of Silver Grass Ash Melting Temperature Using Additives. Int. J. of Renewable Energy Research, 2015, Vol. 5, Iss. 1, pp. 258-265.

[Jandacka 2019] Jandacka, J., Trnka, J., Holubcik, M., Kantova, N. Biodegradable municipal waste to combustion in form of compacted solid fuel. AIP Conf. Proc., 2019, 2118, 030019. https://doi.org/10.1063/1.5114747.

[Kuznetsov 2020] Kuznetsov, E., Nahornyi, V., Krenicky, T. Gas Flow Simulation in The Working Gap of Impulse Gas-barrier Face Seal. Management Systems in Production Engineering, 2020, Vol. 28, No. 4, pp. 298-303.

[Liu 2020] Liu, Z., Ma, R., Xu, G., Wang, W. and Liu, J. Laser Additive Manufacturing of Bimetallic Structure from Ti-6Al-4V to Ti-48Al-2Cr-2Nb via Vanadium Interlayer. Materials Letters, 2020, Vol. 263, 127210.

[Mascenik 2020] Mascenik, J., Pavlenko, S. Determination of stress and deformation during laser welding of aluminium alloys with the PC support. MM Science Journal, 2020, Vol. November, pp. 4104-4107.

[Miglierini 2006] Miglierini, M., et al. Magnetic microstructure of NANOPERM-type nanocrystalline alloys. Physica Status Solidi (B), 2006, Vol. 243, Issue 1, pp. 57-64. DOI: 10.1002/PSSB.200562446.

[Oleksakova 2017] Oleksakova, D., Kollar, P. and Füzer, J. Low Frequency Core Losses Components of FeNiMo Powder Compacted Materials. Acta Physica Polonica A, 2018, Vol. 133, pp. 639-641.

[Oleksakova 2022] Oleksakova, D., et al. Impact of the Surface Irregularities of NiFeMo Compacted Powder Particles on Irreversible Magnetization Processes. Materials, 2022, Vol. 15, No. 24, 8937.

[Onuike 2018] Onuike, B., and Bandyopadhyay, A. Additive Manufacturing of Inconel 718 – Ti6Al4V Bimetallic Structures. Additive Manufacturing, 2018, Vol. 22, pp. 844-851.

[Panchenko 2010] Panchenko, V.Ya., et al. Technologies and Physical Mechanisms of Laser 3D Synthesis of Metallic Powder Materials. In: 10th Int. Conf. Laser and Laser-information Technologies: Fundamental Problem and Applications (ILLA'2009), 18-22 October 2009, Smolyan, Bulgaria; 6th Int. Symp. Laser Technologies and Laser, LTL'2009, Plovdiv, Bulgaria 2010, pp. 122-128. ISSN 1314-068X

[Panda 2021] Panda, A., Anisimov, V.M., Anisimov, V.V., Dyadyura, K. and Pandova, I. Increasing of wear resistance of linear block-polyurethanes by thermal processing methods. MM Science Journal, 2021, No. October, pp. 4731-4735.

[Sebek 2017] Sebek, M., Falat, L., Kovac, F., Petryshynets, I., Hornak, P. and Girman, V. The Effects of Laser Surface Hardening on Microstructural Characteristics and Wear Resistance of AISI H11 Hot Work Tool Steel. Archives of Metallurgy and Materials, 2017, Vol. 62, No. 3, pp. 1721-1726.

[Shishkovsky 2009] Shishkovsky, I.V. Laser synthesis of functionally graded mesostructures and volumetric products. Moscow: Fizmatlit, 2009, 424 p.

[Slovensky 2020] Slovensky, P., et al. Mechanical surface smoothing of micron-sized iron powder for improved silica coating performance as soft magnetic

composites. Applied Surface Science, 2020, Vol. 531, 147340. ISSN 0169-4332

[SMC 2017] Special Metals Corporation (SMC). Inconel alloy 718. [online]. 17 May 2017 [10 January 2024] Available from <https://web.archive.org/web/20170517080338/http://www.specialmetals.com/documents/Inconel%20alloy%20718.pdf>

[Stavertiy 2017] Stavertiy, A.Y. Development and research of technology for growing objects using the method of coaxial laser melting of powder materials. Dissertation for the degree of Candidate of Technical Sciences. 2017.

[Sukhodub 2019] Sukhodub, L., et al. Hydroxyapatite and zinc oxide based two-layer coating, deposited on Ti6Al4V substrate. MM Science Journal, 2019, No. December, pp. 3494-3499.

[Traxel 2020] Traxel, K.D. and Bandyopadhyay, A. Influence of in situ Ceramic Reinforcement Towards Tailoring Titanium Matrix Composites Using Laser-Based Additive Manufacturing. Additive Manufacturing, 2020, Vol. 31, 101004.

[Xu 2020] Xu, J., Yang, M., Ma, H., Shen, Z. and Chen, Z. Fabrication and Performance Studies on Explosively Welded CuCrZr/316L Bimetallic Plate Applied in Extreme Environments. Journal of Materials Research and Technology, 2020, Vol. 9, No. 4, pp. 8971-8984.

[Zajemska 2022] Zajemska, M., Magdziarz, A., Iwaszko, J., Skrzyniarz, M. and Poskart, A. Numerical and experimental analysis of pyrolysis process of RDF containing a high percentage of plastic waste. Fuel, 2022, Vol. 320, 123981.

[Zajemska 2023] Zajemska, M., et al. The role of calorific waste in transformation of iron and steel industry towards sustainable production. Resources, Conservation & Recycling, 2023, Vol. 191, 106899.

[Zhang 1998] Zhang, Y. and Faghri, A. Melting and Solidification of a Subcooled Mixed Powder Bed with Moving Gaussian Heat Source. J. Heat Transfer, 1998, Vol. 120, No. 4, pp. 883-891.

[Zhang 2018] Zhang, Y. and Bandyopadhyay, A. Direct Fabrication of Compositionally Graded Ti-Al2O3 Multi-Material Structures Using Laser Engineered Net Shaping. Additive Manufacturing, 2018, Vol. 21, pp. 104-111.

CONTACTS:
Assoc. Prof. Yevhen Karakash, PhD.
Ukrainian State University of Science and Technologies
Institute of Industrial and Business Technologies
Lazaryana Street 2, Dnipro, 49010, Ukraine
e-mail: yevgenkarakash@gmail.com

Prof. Ing. Miroslav Rimar, CSc.
Assoc. Prof. Ing. Jan Kizek, PhD.
Assoc. Prof. Ing. Marcel Fedak, PhD.
Assist. Prof. Andrii Kulikov, PhD.
Technical University of Kosice
Faculty of Manufacturing Technologies with a seat in Presov
Department of Process Technique
Sturova 31,080 01 Presov, Slovak Republic
tel.: +42155 602 6341, +421 55 602 6329, +421 55 602 6330
miroslav.rimar@tuke.sk; jan.kizek@tuke.sk;
marcel.fedak@tuke.sk; andrii.kulikov@tuke.sk

Assoc. Prof. Olena Karpovych, PhD.
Denys Zhumar
Oles Honchar Dnipro National University
Physical and Technical Faculty
Gagarina Avenue 72, Dnipro, 49010, Ukraine
e-mail: kelvladmail@gmail.com, zhumar82@gmail.com